

# Measurement of $\nu$ -values for TARN by the RF Knock-out Method

A. Noda, T. Hori, K. Chida, T. Hattori,  
T. Katayama, A. Mizobuchi, M. Mutou, T. Nakanishi,  
N. Tokuda, H. Tsujikawa, S. Yamada, M. Yoshizawa,  
S. Watanabe and Y. Hirao

Nov. 1980

*STUDY GROUP OF NUMATRON AND  
HIGH-ENERGY HEAVY-ION PHYSICS  
INSTITUTE FOR NUCLEAR STUDY  
UNIVERSITY OF TOKYO*

*Midori-Cho 3-2-1, Tanashi-Shi,  
Tokyo 188, Japan*

Measurement of  $\nu$ -values for TARN  
by the RF Knock-out Method

A. Noda, T. Hori\*, K. Chida, T. Hattori,  
T. Katayama, A. Mizobuchi, M. Mutou, T. Nakanishi,  
N. Tokuda, H. Tsujikawa, S. Yamada, M. Yoshizawa,  
S. Watanabe and Y. Hirao

Abstract

The number of betatron oscillations per revolution ( $\nu$ -value) can be measured experimentally by an RF knock-out method. The principle of the method is formulated. The RF knock-out system for TARN was designed and constructed. Its design and specifications are described in detail. The experimental results with  $H_2^+$  and  $He^{2+}$  beams with the kinetic energy of 7 MeV/u are compared with the calculation with the computer program SYNCH. The  $\nu_x$  and  $\nu_z$  were measured to be 2.29 and 2.12, respectively, for the excitation currents of the quadrupole magnets;  $I_D = 121$  A ( $G_D = 0.212$  kG/cm) and  $I_F = 74.5$  A ( $G_F = 0.131$  kG/cm). The calculation indicates that the corresponding values are 2.21 and 2.19, respectively, which are in fairly good agreement with the experimental ones.

---

\* On leave from Sumitomo Heavy Industries, Co. Ltd.

## 1. Introduction

TARN (Test Accumulation Ring for the NUMATRON project) was designed by the use of the computer program SYNCH.<sup>1),2)</sup> This program is used in the design of various high energy particle accelerators. It is of great importance to check the calculation experimentally, especially by measuring the  $\nu$ -values in order to ascertain the design principle of the machine. As the methods of measuring  $\nu$ -values, the RF knock-out method<sup>3)</sup> and the one which utilize the Fourier analysis<sup>4)</sup> are known. In our case the beam intensity is quite low, because an SF cyclotron is used as an injector. So the latter is considered to be inconvenient in our case and the RF knock-out method was adopted. At TARN, due to low velocity of accumulated beam, the transverse coherent instability will become severe problem. In order to surmount the instability, the chromaticity control by sextupole magnets are considered.<sup>5)</sup> The  $\nu$ -measurement is also important as the method to judge whether the sextupole correction works well.

In this paper, the general formulation of the RF knock-out method is given in chapter 2. In chapter 3, the details of the construction of the system is described about both mechanical and electrical aspects. Finally the experimental results are given and are discussed in connection with the calculation with SYNCH.

## 2. Principle of the RF Knock-out Method

### 2.1. Resonance Condition

The betatron oscillation is enlarged by an external RF field with such a frequency as resonates with the oscillation. The beam collides with the chamber wall etc, and is lost. By measuring such

a resonance frequency, the  $\nu$ -value can be obtained.

The equation of motion of the free betatron oscillation can be written as

$$\frac{d^2y}{ds^2} + K(s)y = 0 \quad , \quad (1)$$

where  $s$  represents the independent variable along the beam orbit and  $y$  represents the displacement of the beam from the reference orbit.

The solution of the equation (1) can be written as

$$y = \sqrt{\epsilon\beta} \sin(\nu\phi(s) + \delta) \quad (0 < \delta < 2\pi) \quad , \quad (2)$$

where  $\epsilon$  is the beam emittance and  $\beta$  is the beta-function and

$$\phi(s) = \int \frac{ds}{\nu\beta} \quad (3)$$

is a function which increases by  $2\pi$  at every revolution and whose derivative is periodic.<sup>6)</sup> If the time,  $t$ , is used as the independent variable, the equation (1) is transformed to

$$\frac{d^2y}{dt^2} + \nu^2 K(s)y = 0 \quad , \quad (4)$$

where  $v = \frac{ds}{dt}$  is the velocity of the beam. Further if the independent variable is transformed to  $N$  (number of revolutions), then the equation becomes

$$\frac{d^2y}{dN^2} + (2\pi\nu)^2 y = 0 \quad , \quad (5)$$

because the betatron oscillation proceeds  $2\pi\nu$  in phase at every revolution. Between the variables  $t$  and  $N$  the following relation holds:

$$t = \frac{N}{f_r} + t_0, \quad (6)$$

where  $f_r$  is the revolution frequency of the beam and  $t_0$  is the time when the beam starts revolution. If we apply the transverse RF electric field with the angular velocity  $\omega_k = 2\pi f_k$  and the peak amplitude  $V_0$ , between parallel electrodes with the distance  $d$ , then the field strength can be described as  $\frac{V_0}{d} \sin(\omega_k \frac{N}{f_r} + \omega_k t_0 + \delta_0)$  and the forced oscillation can be described as

$$\frac{d^2 y}{dN^2} + (2\pi v)^2 y = \frac{q e V_0}{A m_N \gamma d f_r^2} \sin(\omega_k \frac{N}{f_r} + \delta_1) \quad (7)$$

where  $q$  and  $A$  are charge state and mass number of the ion, respectively  $\gamma$  is usual relativistic kinematical factor,  $m_N$  is the atomic mass unit (931.50 MeV),  $\delta_0$  is the phase of the transverse RF field when it is turned on ( $t = 0$ ) and  $\delta_1 = \omega_k t_0 + \delta_0$ . The special solution of (7) is given by

$$y = C \sin(\omega_k \frac{N}{f_r} + \delta_1), \quad (8)$$

where

$$C = \frac{\left( \frac{q e V_0}{A m_N \gamma d f_r^2} \right)}{(2\pi v)^2 - (\omega_k / f_r)^2} \quad (9)$$

From the equation (9), the resonance condition is given by

$$\frac{\omega_k}{f_r} = 2\pi v. \quad (10)$$

Then the resonance occurs at the frequency of

$$\omega_k = 2\pi\nu f_r \quad (11)$$

and if  $\nu$ -value is given by

$$\nu = n + c \quad (0 \leq c < 1) ,$$

where  $n$  is an integer (in the present case,  $n = 2$ ), then (11) can be written as

$$\omega_k = 2\pi n f_r + 2\pi c f_r \quad . \quad (12)$$

The first term gives the same RF phase for every revolution even if we change the integer  $n$ , so a series of the resonant frequencies are obtained as

$$\omega_k = 2\pi m f_r + 2\pi c f_r \quad (m = 0, 1, 2, \dots) \quad . \quad (13)$$

## 2-2. Emittance Growth by the RF Knock-out

For simplicity, we consider the case of  $m = 0$  and the resonant frequency is given by

$$f_k = c f_r \quad . \quad (14)$$

During a period of the external RF electric field, the beam revolves  $k = 1/c$  turns (for example,  $k = 4$  in the case of  $\nu = 2.25$ ) and the phase of the transverse field when the beam passes at  $i$ -th revolution is given by

$$\phi_i = \phi_0 + \frac{2\pi}{k} i = \phi_0 + 2\pi c i \quad (i = 0, 1, \dots, k-1) \quad , \quad (15)$$

as is illustrated in Fig. 1.

The transverse field changes its phase from  $\phi_i - \frac{\omega_k L}{2v}$  to  $\phi_i + \frac{\omega_k L}{2v}$  during the passage of the beam through parallel electrodes (Fig. 2).

Integrating the equation of motion

$$A m_N \gamma \frac{d^2 y_i}{dt^2} = \frac{q e V_0}{d} \sin(\omega_k t + \delta_0) \quad (16)$$

with respect to  $t$  during the above time interval, the following equation is obtained

$$\left. \frac{dy_i}{dt} \right|_{\text{out}} - \left. \frac{dy_i}{dt} \right|_{\text{in}} = \frac{q e V_0}{A m_N \gamma d} \int_{t_i - \frac{L}{2v}}^{t_i + \frac{L}{2v}} \sin(\omega_k t + \delta_0) dt \quad , \quad (17)$$

where  $L$  is the length of the parallel electrodes. From the relation,

$$\frac{dy_i}{dt} = \frac{ds}{dt} \cdot \frac{dy_i}{ds} = v \frac{dy_i}{ds} \quad , \quad (18)$$

the expression (17) can be rewritten as

$$\left. \frac{dy_i}{ds} \right|_{\text{out}} - \left. \frac{dy_i}{ds} \right|_{\text{in}} = \frac{q e V_0}{A m_N \gamma v d} \int_{t_i - \frac{L}{2v}}^{t_i + \frac{L}{2v}} \sin(\omega_k t + \delta_0) dt. \quad (19)$$

From the above relation,

$$\begin{aligned} \Delta y_i' &\equiv \left. \frac{dy_i}{ds} \right|_{\text{out}} - \left. \frac{dy_i}{ds} \right|_{\text{in}} = \frac{2q e V_0}{\omega_k A m_N \gamma v d} \sin(\omega_k t_i + \delta_0) \sin \frac{\omega_k L}{2v} \\ &= F(q/A, V_0, L, \omega_k, v) \sin(\omega_k t_i + \delta_0) \quad , \quad (20) \end{aligned}$$

where the following notation is used:

$$F(q/A, V_0, L, \omega_k, v) = \frac{2 q e V_0}{\omega_k A m_N \gamma v d} \sin \frac{\omega_k L}{2v} . \quad (21)$$

If the length of the parallel plates  $L$  is negligibly short compared with the wave length of the betatron oscillation, we can estimate the emittance growth of the beam using the equation (20). The beam emittance  $\epsilon$  is represented as follows: <sup>6)</sup>

$$\epsilon = \frac{1}{\beta} [y_i^2 + (\alpha y_i + \beta y_i')^2] = \gamma y_i^2 + 2\alpha y_i y_i' + \beta y_i'^2 , \quad (22)$$

where  $\alpha$ ,  $\beta$  and  $\gamma$  are Twiss parameters. In the  $i$ -th revolution,  $\Delta y_i'$  is given by the equation (20) and the corresponding emittance change,  $\Delta \epsilon_i$  is

$$\begin{aligned} \Delta \epsilon_i &= \frac{1}{\beta} [y_i^2 + (\alpha y_i + \beta (y_i' + \Delta y_i'))^2] - \frac{1}{\beta} [y_i^2 + (\alpha y_i + \beta y_i')^2] \\ &= 2\Delta y_i' (\alpha y_i + \beta y_i') + \beta (\Delta y_i')^2 . \end{aligned} \quad (23)$$

During a period of the transverse RF electric field, total emittance growth of the beam is given by

$$\begin{aligned} \Delta \epsilon &= \sum_{i=0}^{k-1} \Delta \epsilon_i \\ &= \sum_{i=0}^{k-1} [2\Delta y_i' (\alpha y_i + \beta y_i') + \beta (\Delta y_i')^2] . \end{aligned} \quad (24)$$

The amplitude of betatron oscillation at the  $i$ -th revolution,  $y_i$ , can be written as

$$y_i = \sqrt{\epsilon \beta} \sin (2\pi v i + \psi_0) , \quad (25)$$



where  $\psi_0$  is the phase of the betatron oscillation when the beam passes through the parallel electrodes at  $t = t_0$ . From the equation (25) the following relation is easily obtained,

$$y'_i = \sqrt{\epsilon/\beta} [-\alpha \sin(2\pi\nu \cdot i + \psi_0) + \cos(2\pi\nu \cdot i + \psi_0)] . \quad (26)$$

Using the equations (25) and (26), and approximating the summation in equation (24) by time average using integration in a interval of  $2\pi/\omega_k$ , the following equation is obtained:

$$\begin{aligned} \Delta\epsilon = \frac{\omega_k}{2\pi} \int_0^{2\pi/\omega_k} [ 2F \sin(\omega_k t + \delta_0) \sqrt{\epsilon\beta} \cos(2\pi\nu i + \psi_0) \\ + \beta F^2 \sin^2(\omega_k t + \delta_0) ] dt . \end{aligned} \quad (27)$$

Evaluating the integral for the case where the resonance condition (14) is satisfied, we obtained the following result:

$$\Delta\epsilon = F \sin(\phi_0 - \psi_0) \sqrt{\epsilon\beta} + \frac{1}{2} \beta F^2 , \quad (28)$$

because the following relation exists:

$$\begin{aligned} \omega_k t + \delta_0 &= \phi_i \\ &= \phi_0 + 2\pi c i . \end{aligned} \quad (29)$$

Therefore the following relation is obtained:

$$\frac{d\varepsilon}{dz} = F \sin(\phi_0 - \psi_0) \sqrt{\varepsilon\beta} + \frac{1}{2} \beta F^2. \quad (30)$$

Using the transformation,

$$x = \sqrt{\varepsilon}, \quad (31)$$

and the relation,

$$\frac{dx}{dz} = \frac{1}{2x} \frac{d\varepsilon}{dz}, \quad (32)$$

we obtain the next relation:

$$\frac{dx}{dz} = \frac{1}{2} \sqrt{\beta} F \sin(\phi_0 - \psi_0) + \frac{\beta F^2}{4} \frac{1}{x}. \quad (33)$$

About the first term of the expression (33), the  $z$ -dependence of  $x = \sqrt{\varepsilon}$  is linear, but from the second term of (33), the following dependence is expected,

$$x = \sqrt{\varepsilon} \propto \sqrt{z} \quad (34)$$

so, in the case of  $\sin(\phi_0 - \psi_0) \neq 0$ , the first term of (33) is the leading term and from the relation

$$\frac{dx}{dz} = \frac{1}{2} \sqrt{\beta} F \sin(\phi_0 - \psi_0) \quad (35)$$

the growth rate of the amplitude of the betatron oscillation is

$$\Delta a = \frac{1}{2} F \beta \sin (\phi_0 - \psi_0) z \quad . \quad (36)$$

But for the case where the initial phase difference,  $\phi_0 - \psi_0$ , between the betatron oscillation and the external RF electric field has the condition of

$$\sin (\phi_0 - \psi_0) = 0 \quad , \quad (37)$$

the equation (33) becomes

$$\frac{dx}{dz} = \frac{\beta F^2}{4} \frac{1}{x} \quad . \quad (38)$$

The solution of this equation is

$$\dot{x} = \frac{\beta F^2}{2} z \quad . \quad (39)$$

Hence the growth rate of the amplitude is

$$\Delta a = \frac{1}{\sqrt{2}} \beta F \sqrt{z} \quad . \quad (40)$$

### 3 Construction of the RF Knock-out System for TARN

#### 3-1 Required Condition

TARN aims at the accumulation of  $N^{5+}$  beam with the kinetic energy of 8.55 MeV/u. An RF knock-out system is designed to give enough deflection to  $N^{5+}$ , because it is considered to be most serious case.

#### a) Resonance Frequency of the Transverse RF Electric Field

From the relation (14), the resonant frequency is obtained for

the  $\nu$ -value of 2.10  $\sim$  2.50 to be

$$100 \text{ kHz} < f_k < 650 \text{ kHz} ,$$

as  $f_r = 1.27 \text{ MHz}$  in this case.

b) Necessary Voltage for the Transverse RF Field

The initial phase of the betatron oscillation of the beam, which is injected into full acceptance by multi-turn mode, has a spread as large as  $\pi$ . The particle which has such an initial phase as satisfies the relation of

$$\sin(\phi_0 - \psi_0) = 1 , \quad (41)$$

is kicked out at first. For these particles, the growth rate of the amplitude of the betatron oscillation is

$$\Delta a = \frac{1}{2} F \beta z' = \frac{\beta z' q e V_0}{\omega_k A m \gamma v d} \sin \frac{\omega_k L}{2v} . \quad (42)$$

In the present case, the numerical values are as follows:

$$\beta \approx \begin{cases} 2.3 \text{ m} & (\text{in horizontal direction : H.D.}) \\ 2.8 \text{ m} & (\text{in vertical direction : V.D.}) \end{cases}$$

$$q/A = \frac{5}{14} = 0.357 \quad (43)$$

$$\gamma = 1.00918$$

$$v = 4.04 \times 10^7 \text{ m/sec}$$

and the dimensions of the electrodes are

$$\begin{aligned}
 d &\approx \begin{cases} 0.20 \text{ m} & \text{(H.D.)} \\ 0.06 \text{ m} & \text{(V.D.)} \end{cases} \\
 L &\approx \begin{cases} 0.30 \text{ m} & \text{(H.D.)} \\ 0.125 \text{ m} & \text{(V.D.)} \end{cases} ,
 \end{aligned} \tag{44}$$

the details of which are described in the next section.

For the case of  $v = 2.25$  (our design value is around this value),  $\frac{\omega_k L}{2v} = 0.0074$  for H.D. and  $0.0031$  for V.D. and for both case  $\frac{\omega_k L}{2v} \ll 1$ , then

$$\sin \frac{\omega_k L}{2v} \approx \frac{\omega_k L}{2v} . \tag{45}$$

Therefore the equation (42) becomes

$$\Delta a = \frac{\beta \cdot i}{2} \cdot \frac{q e V_o L}{A m_N \gamma v^2 d} . \tag{46}$$

The beam will be lost when the amplitude grows as large as  $d/2$  and if we want to kick out the beam within  $N_o$  turns, the required voltage is

$$V_o = \frac{A m_N \gamma v^2 d^2}{q e L \beta N_o} . \tag{47}$$

For the numerical values given above, the required voltage are

$$V_o = \begin{cases} 2.77 \times 10^6 / N_o & \text{Volts (H.D.)} \\ 0.491 \times 10^6 / N_o & \text{Volts (V.D.)} \end{cases} \tag{48}$$

and if we want to kick out the beam within 5,000 turns, necessary voltage is

$$V_0 = \begin{cases} 0.553 & \text{kV (H.D.)} \\ 0.0982 & \text{kV (V.D.)} \end{cases} \quad (49)$$

As the extreme case, for the particle which has an initial phase as satisfies  $\sin(\phi_0 - \phi_0) = 0$ , the first term in the right-hand side of the relation (33) disappears and the amplitude growth is given by the equation (40). In order to attain the amplitude growth of  $d/2$  in  $N_0$  turns, the necessary voltage is

$$V_0 = \frac{Am_N \gamma v^2 d^2}{\sqrt{2} q e L \beta \sqrt{N_0}}, \quad (50)$$

which gives the following relation in the present case,

$$V_0 = \begin{cases} 1.96 \times 10^6 / \sqrt{N_0} & \text{Volts (H.D.)} \\ 0.347 \times 10^6 / \sqrt{N_0} & \text{Volts (V.D.)} \end{cases} \quad (51)$$

In the case where the voltage given by Eq. (49) is applied, the required turn number until the necessary amplitude growth is given is

$$N_0 = 1.26 \times 10^7 \quad \text{turns} \quad (52)$$

for both directions. This turn number corresponds the time interval of almost 10 seconds. In real case, the beams are kicked out continuously from the particle which satisfies the equation (41).

From the above consideration, the transverse RF electric field should have the following characteristics,

|                 |                |      |
|-----------------|----------------|------|
| Frequency range | 0.1 ~ 1.0 MHz  | (53) |
| Peak voltage    | above 0.7 kV , |      |

where some margin is considered in the peak voltage.

### 3-2 Mechanical Construction of Electric Plates and Vacuum Chamber

The electrodes should be installed in a vacuum chamber in which the pressure is about  $8 \times 10^{-11}$  Torr. No organic material can be used for the fabrication. The plates are made of 2 mm thick copper with low oxide from the consideration of outgassing. The dimensions of the plates illustrated in Fig. 3 are determined to ensure the sufficient aperture for the beam, say 195 mm and 45 mm in horizontal and vertical directions, respectively. The length of the plates determined from the available free space of the TARN are 300 mm and 125 mm for horizontal and vertical measurements, respectively. These plates are fixed symmetrically about the central orbit by four 10 mm thick ceramic discs with rectangular hole in the center to insulate the plates from the chamber. The total view of the electrodes is shown in Fig. 4.

As the feedthrough of the RF power, the N type connectors with ceramic insulators are used.<sup>8)</sup> Coaxial cables with the insulation of ceramic beads are used to link the connectors with the electric plates. Figure 5 shows the feedthrough and the coaxial cables.

The vacuum chamber is made of stainless steel SUS 316L, whose

inner diameter is 343 mm. The vacuum chamber for RF knock-out is installed in TARN after it was backed up to around 300° centigrade and pumped down to  $\sim 1 \times 10^{-10}$  Torr at a test stand. The overall view of the test stand is shown in Fig. 6. The chamber is installed in the straight section, S7, of TARN as illustrated in Fig. 7. The overall view of the installed RF knock-out chamber is shown in Fig. 8.

### 3-3 Electronics System to Feed the Transverse RF Field

As described in the previous section, we want to apply an RF field with the frequency range between 0.1 ~ 1.0 MHz and the maximum peak voltage 0.7 kV (1.4 kV peak to peak voltage: denoted as  $V_{p-p}$  hereafter). A function generator with a voltage controlled oscillator (HP 3312A) which can provide a 10 V peak to peak signal to a 50 ohms load in the frequency range from 0.1 Hz to 13 MHz. In order to apply  $V_{p-p}$  of 1.4 kV, a power amplifier is used (R&K A3050). To minimize the required power, we used series resonance. Inductance coils are connected in series to the capacitor of the parallel plates (0.4 pF in horizontal and 4 pF in vertical), and the vacuum condenser with variable capacitance from 0 to 50 pF is used in parallel with the electrodes as illustrated in Fig. 9, where the block diagram of the electronics system is also shown. In Fig. 10, the vacuum condenser and the inductance coils are shown. The vacuum condenser is connected with a pulse motor and a helical potentiometer. The capacitance can be controlled remotely from the control room by the use of a pulse motor controller.<sup>9)</sup> The capacitance of the vacuum condenser is monitored by the helical potentiometer. The inductance of each coil



is about 180  $\mu\text{H}$  and the number of coils are changed (2 and 4 in horizontal and vertical measurements, respectively) according to the frequency range.

An analog switch is used in order to feed pulsed RF for a short interval so as to measure  $\nu$ -values at the various orbits. As is shown in Fig. 11, the timing pulse is fed from the circuit to fire the kicker magnet in the transport line.<sup>10)</sup> The typical timing chart is shown in Fig. 12 in connection with another timings.

The resonance curves of the circuit above mentioned are shown in Fig. 13 both for horizontal and vertical ones. From the consideration of the Q value of the system ( $\sim 10$ ) and the required voltage for the external field, the output power of the amplifier was designed to be 50 W. The amplifier has a wide frequency range from 100 kHz to 27 MHz and has a large gain of 45 dB, and in reality it could provide a power as large as 100 W in the higher frequency range. It also has a variable attenuator and a protection circuit for short or open of the output, which is found to be useful especially for the laboratory use.

#### 4 Measurement of $\nu$ -values for TARN

##### 4-1 Numerical Calculation for $\text{H}_2^+$ and $\text{He}^{2+}$

Beam injection and RF stacking have been executed from August of 1979 with the use of molecular hydrogen ( $\text{H}_2^+$ ) and helium ( $\text{He}^{2+}$ ) beam accelerated up to 7 MeV/u by the SF cyclotron at INS. For this case, the numerical values which differ from the ones in equation (43) are as follows:

$$q/A = 0.5$$

$$\gamma = 1.0075 \quad (54)$$

$$v = 3.66 \times 10^7 \text{ m/sec}$$

and other values are the same as the ones given in 3-1. (Strictly speaking,  $m_N$  should be modified to be 938 MeV for molecular hydrogen ( $H_2^+$ ), but the mass difference due to coupling is neglected for simplicity.) Therefore the following relations are obtained instead of Eq. (48),

$$V_0 = \begin{cases} 1.62 \times 10^6/N_0 & \text{(Volts) (H.D.)} \\ 0.287 \times 10^6/N_0 & \text{(Volts) (V.D.)} \end{cases} \quad (55)$$

for the particles which have an initial phase as satisfies Eq. (41). If a transverse RF field with the peak voltage of 0.7 kV ( $V_{p-p}$  of 1.4 kV) is applied, the beam will be kicked out after about 2300 and 400 revolutions for horizontal and vertical directions, respectively, which correspond to the times about 2 ms and 0.3 ms, respectively.

#### 4-2 Experimental Results and Discussion

The molecular hydrogen beam ( $H_2^+$ ) with a kinetic energy of 7 MeV/u is injected into the TARN by a multi-turn injection method. The magnetic rigidity of the injected beam is measured to be

$$B \cdot \rho = 768.0 \text{ kG} \cdot \text{cm} \quad (56)$$

and the frequency of the accelerating RF field (not for knock-out but for RF acceleration in order to stack the beam into the inner side

of the ring) which synchronizes with the injected beam is

$$f_{rf} = 7.987 \text{ MHz.} \quad (57)$$

The harmonic number ,h, of the RF system is seven, so the revolution frequency of the beam ,f<sub>r</sub>, is obtained from the relation,

$$f_r = \frac{1}{h} f_{rf} = \frac{1}{7} f_{rf} \quad (58)$$

and is equal to 1.141 MHz for the injected beam. From Eq. (56), the momentum of the injected beam is calculated at 230.4 MeV/c by the following relation

$$pc = 0.3 B \cdot \rho \quad (\text{MeV}) \quad . \quad (59)$$

The ratio of the velocity of the beam to that of light,β, is calculated at 0.1219 and the total length of the injection orbit is estimated at 32.04 m.

At the accumulation of the beam, the fields of the bending magnets are set to be 5.627 kG. The radius of curvature of the central orbit (ρ<sub>0</sub>) is given by the relation,

$$N_B L_B = 2\pi\rho_0 \quad , \quad (60)$$

where N<sub>B</sub> and L<sub>B</sub> are the number of dipole magnets,8, and their effective length, respectively. From the field measurement, L<sub>B</sub> is 104.5 cm, therefore ρ<sub>0</sub> = 133.0 cm. Hence in the above condition, the central magnetic rigidity is

$$B \cdot \rho_0 = 748.4 \text{ kG} \cdot \text{cm} \quad (61)$$

and the injected beam has a fractional momentum difference ( $\Delta p/p_0$ ) of 2.62 % from the central one. In the experiment, the RF acceleration frequency is swept, and between  $\Delta f/f_0$  and  $\Delta p/p_0$ , the following relation exists:

$$\frac{\Delta f}{f_0} = \left( \frac{1}{\gamma^2} - \frac{1}{\gamma_t^2} \right) \frac{\Delta p}{p_0}, \quad (62)$$

where  $\gamma_t$  is the transition  $\gamma$ . The value in the parentheses changes from orbit to orbit and the equation (62) is represented in Fig. 14 using the calculated  $\gamma_t$  by SYNCH. From the figure, the fractional revolution frequency,  $\frac{\Delta f}{f_0}$ , is 1.89 % at the injection orbit, which corresponds to the fractional momentum,  $\frac{\Delta p}{p_0}$ , of 2.62 %. From the above consideration, the beam circulating along the central orbit has a revolution frequency of

$$f_{r_0} = \frac{1}{7} \frac{7.987}{1.0189} \text{ MHz} = 1.120 \text{ MHz} \quad (63)$$

In Fig. 15, the  $v$ -value calculated by SYNCH is shown with solid lines for various closed orbits for the corresponding fractional momenta between 0.0 % and +3.0 %, and in Fig. 16, the calculated work line of the operation is given by the line B. In the calculation, the results of the magnetic field measurement were taken into account<sup>5)</sup>.

The beam signal is picked up by an electrostatic monitor installed in the S3 section of Fig. 7 and selectively amplified by a resonance amplifier<sup>11)</sup>. The output signal of the amplifier is observed together with the high voltage signal between electrodes by a synchroscope. The experimental

measurement is illustrated in Fig. 17 (a) ~ (e). In the example, the RF acceleration is not applied and the  $\nu$ -value in the horizontal direction is measured at the injection orbit. As is easily observed, the betatron oscillation in the horizontal direction resonates with the transverse RF electric field at the frequency 359.3 kHz, where the beam is kicked out within 0.5 msec (less than 600 turns) by the RF voltage 2 kV peak to peak.

According to Eq. (55), it is expected the beam is lost in about 1600 turns, which is longer than the experimental results. The difference is understood as follows. In the calculation, the beam is assumed to be lost for the first time when its amplitude grew as large as 10 cm where the parallel plates for horizontal measurement locate. In reality, however, when the beam deviate as large as 7 cm from the central orbit, it will be lost by collision with the electrostatic beam monitor. Further the injection orbit is  $\sim 2$  cm outer from the central orbit, and the beam will be lost when its amplitude grows as large as 5 cm. Taking this condition into account, the estimated turn number of the beam before it is lost is  $\sim 800$  turns, which seems in good agreement with the experimental value.

From the resonant frequency  $f_k$  of 359.3 kHz and the Eq. (14), we obtain 0.315 as the value of  $c$ , and then  $\nu_x$  is 2.315 believing the value of  $n$  calculated by SYNCH for the currents of  $I_F = 76$  A and  $I_D = 121$  A, where  $I_F$  and  $I_D$  mean the excitation currents of radially focusing and defocusing quadrupole magnets, respectively. The resolution of  $f_k$  is better than 3 kHz as is easily known from Fig. 17 and the accuracy of  $\nu$  value is better than 0.0004.

For the measurement of  $\nu$ -values at the stacked orbits, the pulsed RF is applied changing its timing by a delay circuit just before

the analog switch as is shown in Fig. 18 (a). The behavior of the beam when the pulsed RF is applied is shown in Fig. 18(b). In these measurements the excitation current of the quadrupole magnets are set to be  $I_F = 74.5A$  and  $I_D = 121A$ . By the measurement, the  $\nu$ -values at such stacked orbits are obtained experimentally for both  $\nu_x$  and  $\nu_z$ . The results are given in Fig. 15 (a), (b) by the open circles and they are also listed up in Table.

The chromaticity which is defined as

$$\xi \equiv \partial\nu/\partial\left(\frac{\Delta P}{P}\right) \quad (64)$$

are calculated to be  $-6.63$  and  $-0.27$  in horizontal and vertical directions, respectively, near the central orbit, and the experimentally obtained ones are  $-1.59$  and  $-0.47$ . In horizontal direction the size of the chromaticity is small compared with the calculation. In vertical direction, the  $\nu_z$  is  $0.07$  smaller than the calculation but its momentum dependence is quite similar to the calculation.

#### Acknowledgement

The authors would like to express their sincere thanks to Dr. Al. Garren at LBL, who joined them from March to June, 1979, and made the great contribution on chromaticity correction. He also brought with him the newest version of SYNCH. One of the authors (A. Noda) would like to express his thanks to Dr. T. Miyahara at Tokyo Metropolitan University for his communication about the RF knock-out method. The numerical calculation with computer code SYNCH was executed by FACOM M 180 II AD at INS. One of the authors (A. Noda) is also grateful to Mr. K. Chiba

of the computer room at INS for his conversion of the program SYNCH for our machine. The authors are grateful to Profs. K. Sugimoto and M. Sakai for their continuous encouragements.

#### References

1. A. Garren and J. W. Eusebio, "A Computer System for Synchrotron Design and Orbit Analysis", Lawrence Radiation Laboratory preprint, UCID-10154 (1965).
2. A. Noda et al., "Lattice Structure and Magnet Design for the TEST RING", Proc. of 2nd Sym. on Acc. Scie. & Tech. (1978) 83.
3. Y. Miyahara et al., "Measurement of the Betatron Oscillation Frequency in the Booster by the RF Knock-out Method", KEK-76-16 (1977).
4. K. Hübner, "Excitations of Coherent Betatron Oscillations for Q-Measurements", CERN-INS-TH/69-17 (1969).
5. A. Garren and A. Noda, "A Sextupole Magnet Correction System for TARN", INS-NUMA-14 (1979).
6. E. D. Courant and H. S. Snyder, "Theory of the Alternating Gradient Synchrotron", Ann. Phys. 3 (1958) 1.
7. T. Katayama, A. Noda and Y. Hirao, "NUMATRON and TARN", INS-NUMA-17 (1980).
8. H. Ishimaru, "Coaxial, Multi-pin, and Combined Multi-pin and Coaxial Vacuum Feedthrough", Vacuum 21 (1978) 1 (in Japanese).
9. M. Yoshizawa, "A Pulse Motor Controller", to be published in INS-NUMA.
10. S. Watanabe, "TARN Control System", INS-NUMA-26 (1980).
11. N. Tokuda and S. Watanabe, "Electrostatic and Ferrite Core Monitors in the TARN", INS-NUMA-21 (1980).

Table

| Horizontal ( $v_x$ ) |                          |                          |             |       | Vertical ( $v_z$ ) |                          |                          |             |       |
|----------------------|--------------------------|--------------------------|-------------|-------|--------------------|--------------------------|--------------------------|-------------|-------|
| $f_{rf}$ (MHz)       | $\frac{\Delta f}{f}$ (%) | $\frac{\Delta p}{p}$ (%) | $f_k$ (kHz) | $v$   | $f_{rf}$ (MHz)     | $\frac{\Delta f}{f}$ (%) | $\frac{\Delta p}{p}$ (%) | $f_k$ (kHz) | $v$   |
| 7.987                | 1.89                     | 2.62                     | 330         | 2.289 | 7.984              | 1.89                     | 2.62                     | 132         | 2.116 |
| 7.968                | 1.64                     | 2.25                     | 337         | 2.296 | 7.970              | 1.68                     | 2.30                     | 131         | 2.115 |
| 7.947                | 1.38                     | 1.90                     | 342         | 2.301 | 7.961              | 1.56                     | 2.14                     | 131         | 2.115 |
| 7.928                | 1.13                     | 1.57                     | 347         | 2.306 | 7.938              | 1.26                     | 1.75                     | 131         | 2.116 |
| 7.908                | 0.88                     | 1.22                     | 352         | 2.312 | 7.915              | 0.97                     | 1.34                     | 131         | 2.116 |
| 7.888                | 0.63                     | 0.87                     | 358         | 2.318 | 7.892              | 0.67                     | 0.93                     | 134         | 2.119 |
| 7.868                | 0.38                     | 0.53                     | 363         | 2.323 | 7.868              | 0.38                     | 0.53                     | 134         | 2.119 |
|                      |                          |                          |             |       | 7.845              | 0.08                     | 0.12                     | 138         | 2.123 |



## Figure Captions

- Fig. 1 The phase of the transverse RF field for knock-out is illustrated.  $\phi_i$  indicates the phase when the beam passes the center of the electrodes after  $i$ -th revolution.
- Fig. 2 The phase change of the transverse RF field for knock-out during the beam passes through parallel electrodes. It takes the time interval of  $\frac{L}{v}$  for the beam with velocity  $v$  to pass through the electrodes of the length  $L$ . The phase change during this time interval is taken into account.
- Fig. 3 Schematic view of the RF knock-out chamber and electrodes. The lengths of electrodes for horizontal and vertical measurements are 300 mm and 125 mm, respectively. The gap of the electrodes for horizontal measurement is larger (200 mm) compared with that of vertical measurement (60 mm) and the length of the former electrodes is made larger than the latter.
- Fig. 4 Total view of the electrodes installed in the vacuum chamber.
- Fig. 5 The feedthrough and coaxial cables for the RF power. As the feedthrough, N type connector with ceramic insulator is used and the coaxial cable uses the ceramic beads as an insulator considering the temperature rise at the case of baking.
- Fig. 6 The overall view of the test stand for vacuum pumping. A turbo-molecular pump with the pumping speed of 200  $\ell$ /sec is used and after the baking up to around 300° centigrade during around a whole day, the vacuum pressure of  $\sim 1 \times 10^{-10}$  Torr is attained.
- Fig. 7 Total layout of TARN. The RF knock-out chamber is installed in

the S7 section. The behaviour of the beam is monitored by the electrostatic pick-up installed in the S3 section.

Fig. 8 The overall view of the RF knock-out chamber installed in the S7 section.

Fig. 9 The diagram of the electric circuit for the transverse RF for knock-out. A series resonance is used and in order to adjust the peak frequency of resonance, a vacuum condenser (Cv) is used.

Fig. 10 The overall view of the inductance coils (upper) and the vacuum condenser (lower). The vacuum condenser is linked to a pulse motor and a helical potentiometer and can be controlled and monitored from the control room.

Fig. 11 Block diagram of the RF knock-out system. A timing pulse for the pulsed RF for the measurement of the  $\nu$ -values at the stacked orbits are fed from the circuit to trigger the kicker magnet in the transport line, making the time delay as large as  $\tau_d$  by the use of a delay circuit (RF-KO Delay). A variable DC voltage (Frequency Controller) is fed to a voltage controlled oscillator in order to enable fine tuning of the frequency of a signal generator.

Fig. 12 A typical timing chart of TARN. The pulsed RF for knock-out is triggered after the time delay of  $\tau_d$  from the trigger pulse for the kicker magnet. The value of  $\tau_d$  can be varied by the RF-KO delay circuit.

Fig. 13 Typical resonance curves for horizontal and vertical measurement systems when the vacuum condenser is fixed at a certain

value. As is known from the figure, the Q-value of the resonance circuit is about 10.

- Fig. 14 The correlation between the fractional momentum ( $\frac{\Delta p}{p}$ ) and the fractional revolution frequency ( $\frac{\Delta f}{f}$ ) calculated by SYNCH.
- Fig. 15  $\nu$ -values for various fractional momenta. (a)  $\nu$ -value in horizontal direction, (b)  $\nu$ -values in vertical direction. Solid lines represent the calculation by SYNCH and open circles give the measured values by an RF knock-out method.
- Fig. 16 The work line for TARN calculated by SYNCH. Line A indicates the work line when the ideal magnet system exists and the line B is the calculation including the results of field measurements. Other lines ( $L \sim S$ ) are candidates for the work line when the sextupole magnets are used.
- Fig. 17 The beam signal from the electrostatic monitor (upper) and the applied transverse pulsed RF for knock-out (lower). Horizontal scale is 1 ms/div. and vertical scale is 10 mV/div. for upper signal and 500 V/div. for lower signal. The frequencies for the applied transverse pulsed RF are (a) 353.0 kHz, (b) 356.1 kHz, (c) 359.3 kHz, (d) 362.5 kHz and (e) 365.0 kHz. It is known that the betatron oscillation in horizontal direction resonates with the applied RF with the frequency of around 359 kHz. At the measurement, the excitation currents of the quadrupole magnets are  $I_F = 76$  A and  $I_D = 121$  A. As is known from the figure, the resolution of the resonant frequency is better than 3 kHz, which corresponds the resolution of  $\nu$  of the size 0.0004.

Fig. 18 (a) Sweep signal of the frequency of the RF for stacking (upper) and the relative timing of the pulsed RF for knock-out (lower). The RF frequency for stacking is 7.987 MHz at the base line and is 7.841 MHz at the flat top.

(b) The beam signal from the electrostatic monitor (upper) and the transverse pulsed RF applied to the electrodes for knock-out (lower). At these measurement, the excitation currents of the quadrupole magnets are  $I_F = 74.5$  A and  $I_D = 121$  A. Horizontal scale is 5 ms/div. and vertical scale for the pulsed RF is 500 V/div. in both pictures. Vertical scale for the beam signal in (b) is 5 mV/div.

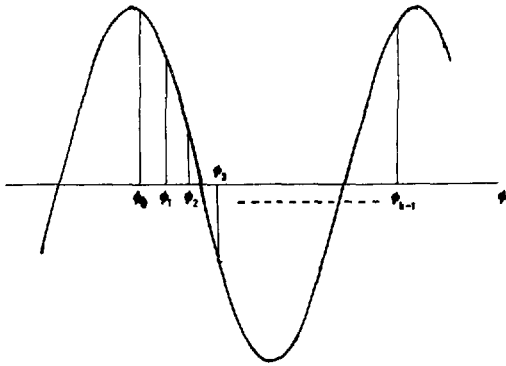


Fig. 1

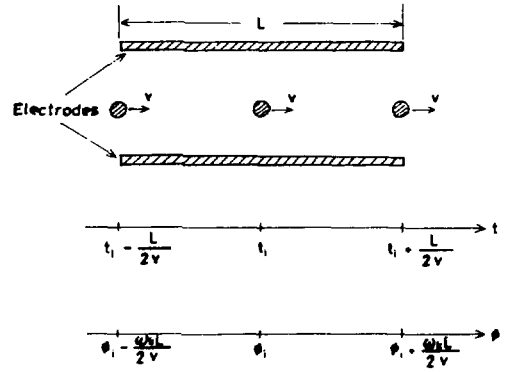


Fig. 2

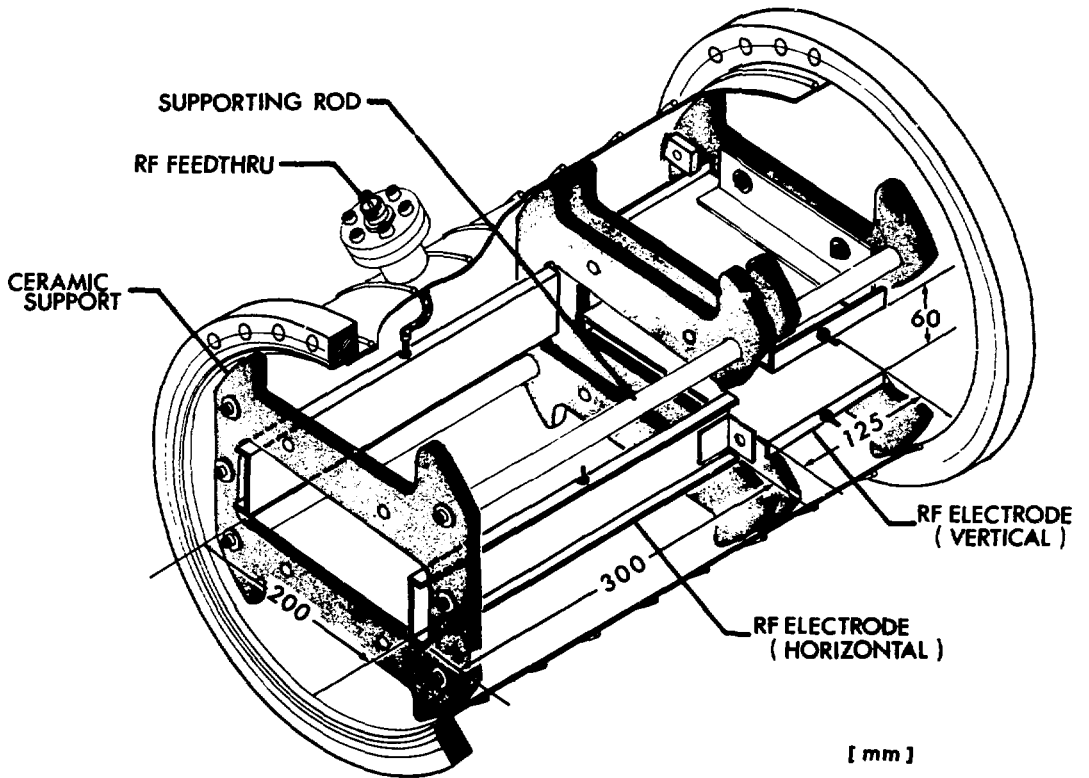


Fig. 3

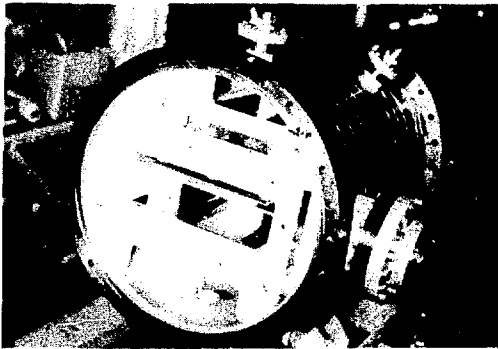


Fig. 4

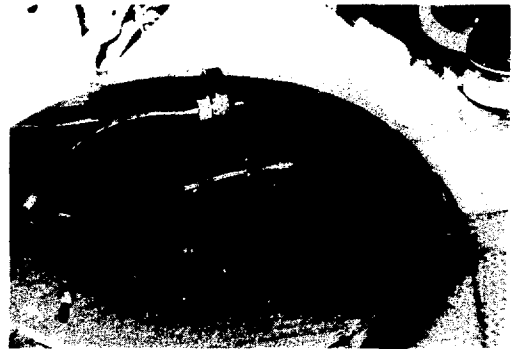


Fig. 5

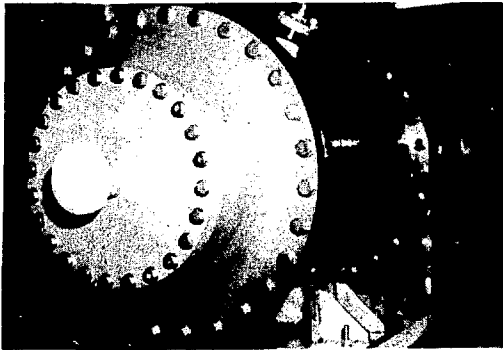


Fig. 6



Fig. 8

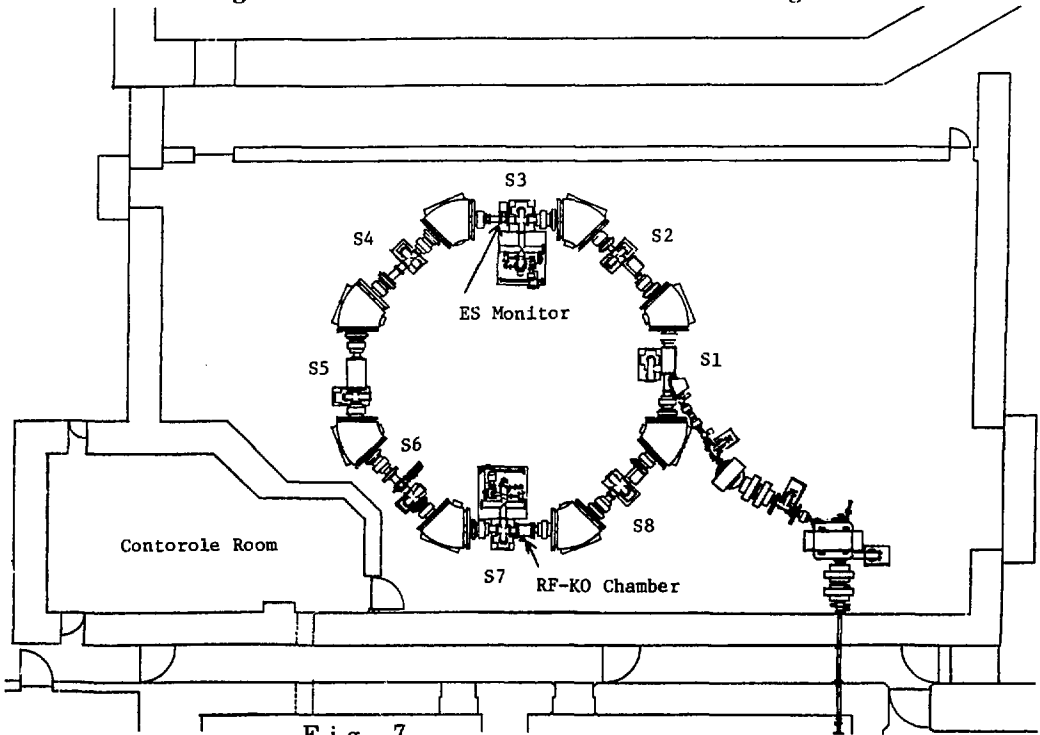
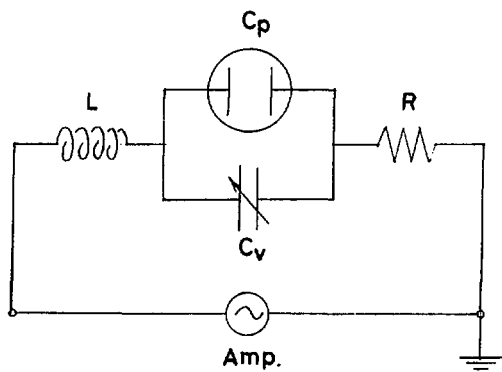


Fig. 7

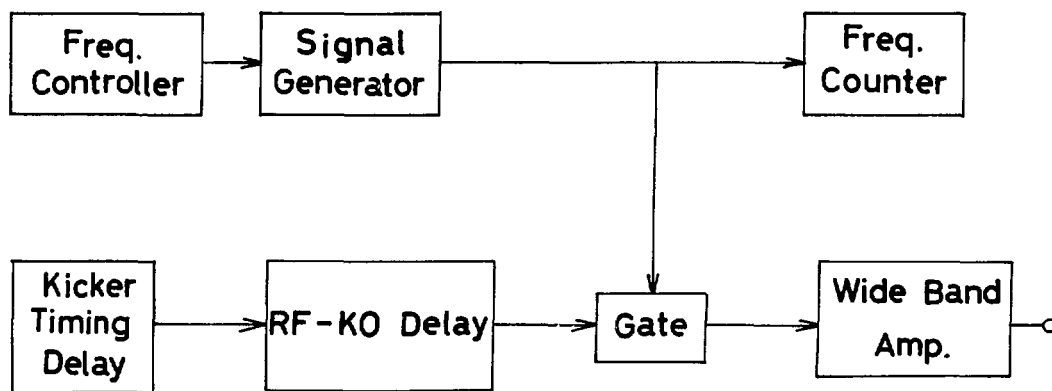


RF-KO Resonance Circuit

Fig. 9



Fig. 10



Block Diagram of RF-KO System

Fig. 11

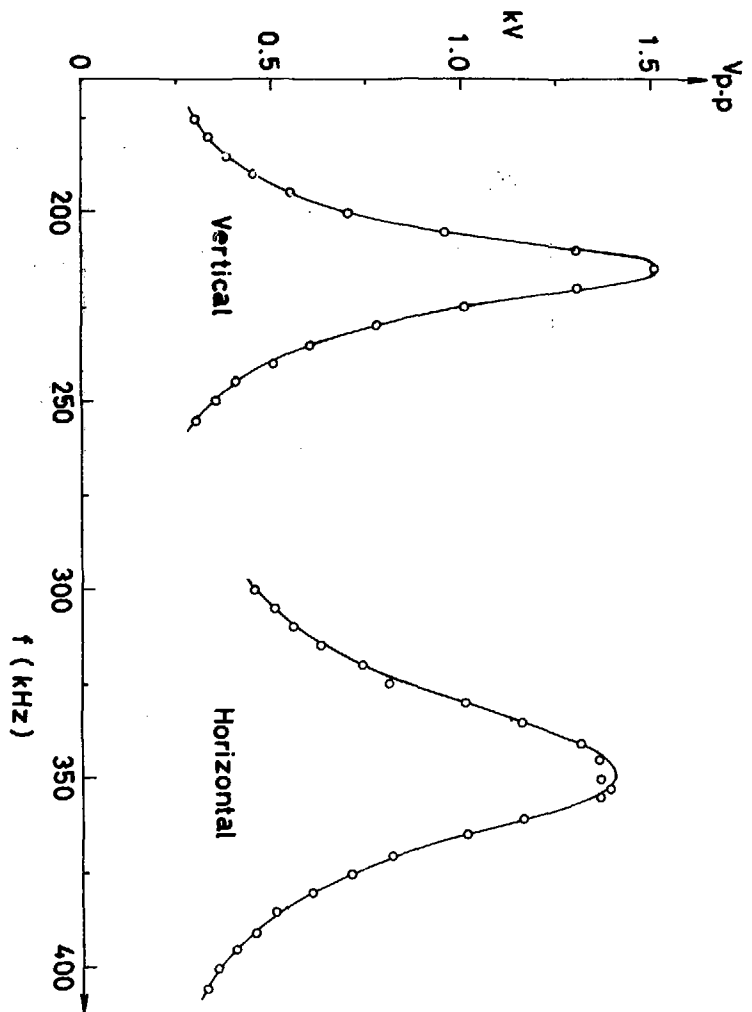


Fig. 13

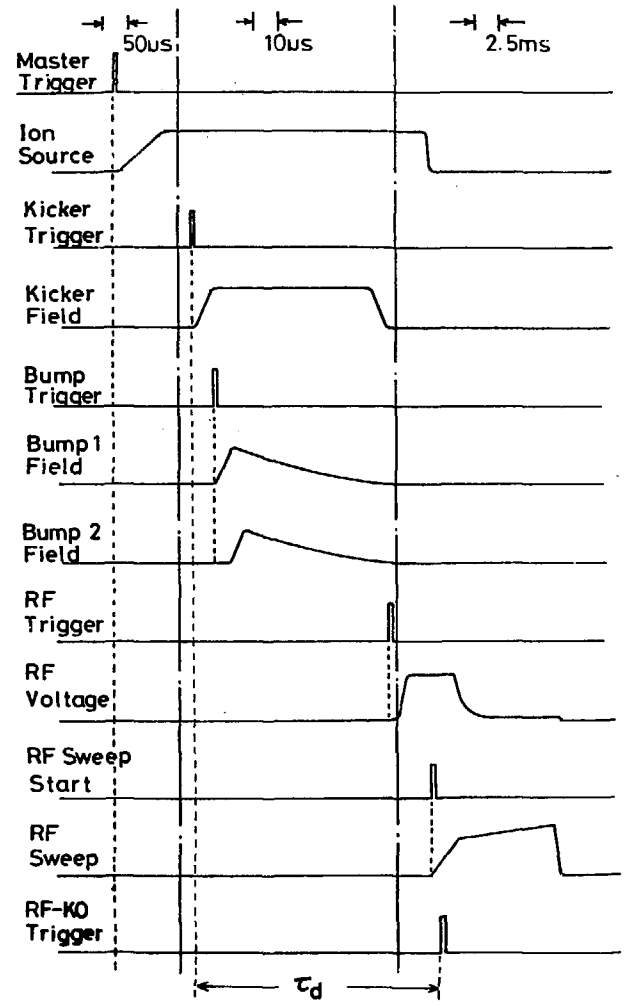


Fig. 12



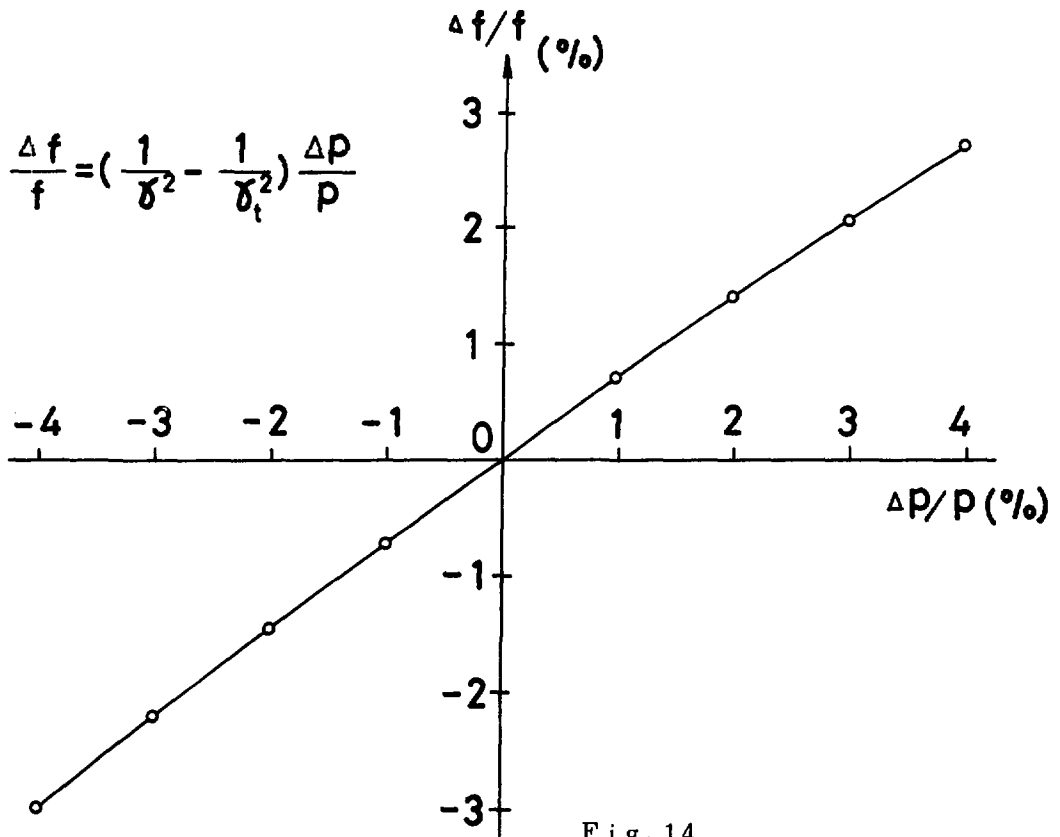


Fig. 14

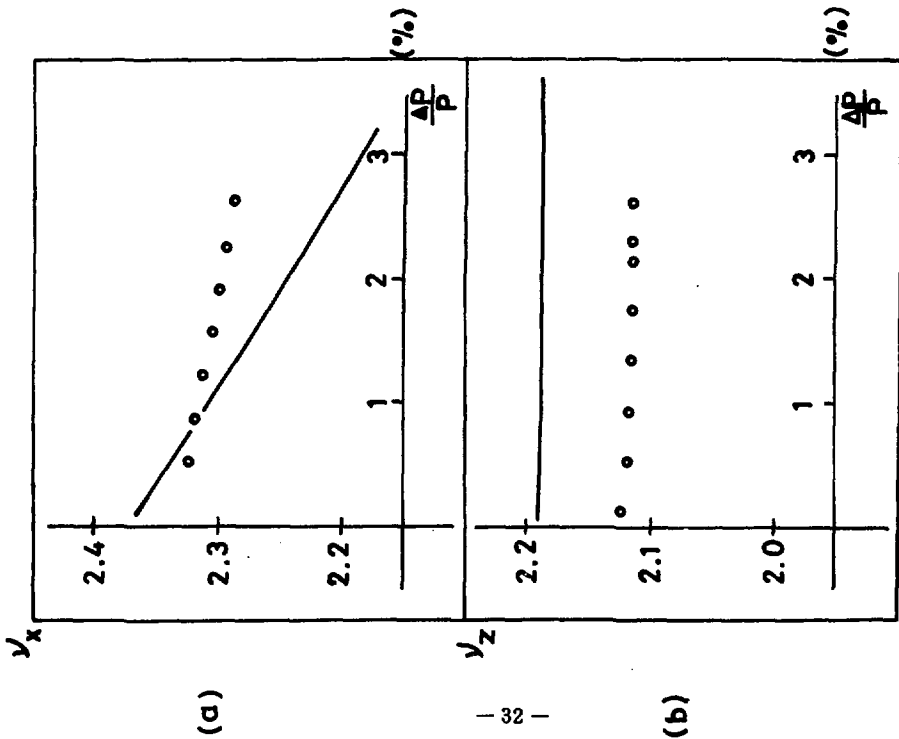
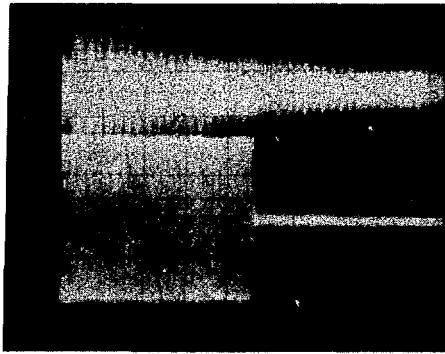
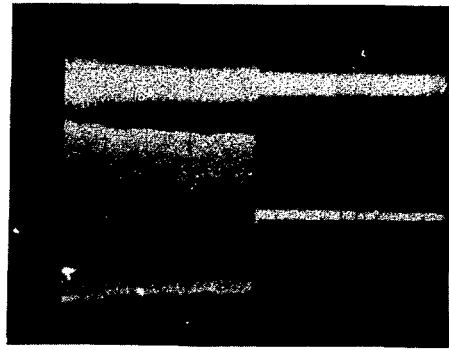


Fig. 15

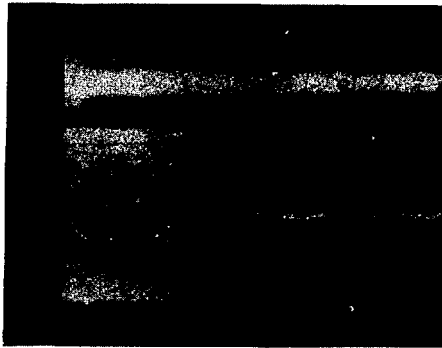




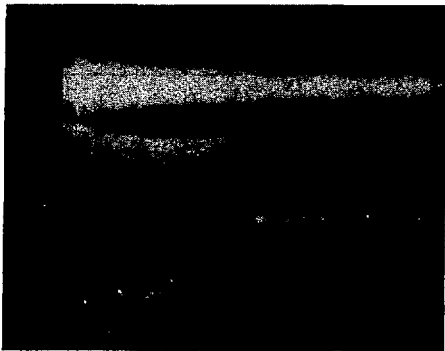
(a)



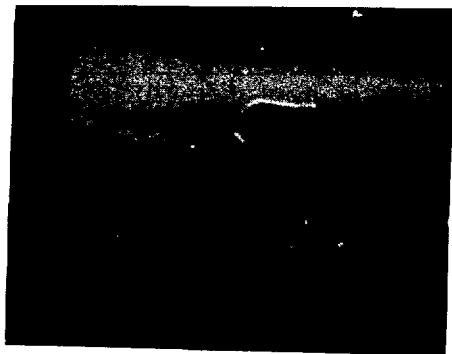
(b)



(c)

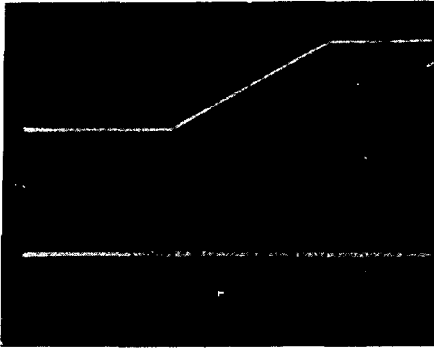


(d)

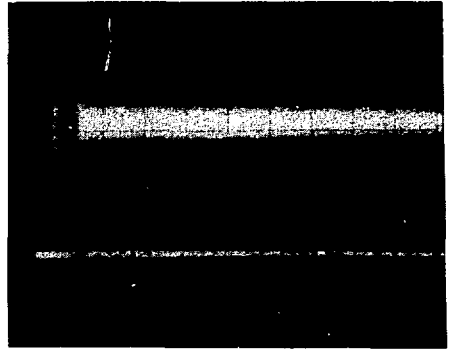


(e)

Fig. 17



(a)



(b)

Fig. 18